Astron. Astrophys. 322, 381–390 (1997)

ASTRONOMY AND ASTROPHYSICS

Molecular gas in the warped galaxy NGC 4013

Ana I. Gómez de Castro[1] **and S. García-Burillo**[2]

[1] Departamento de Astronomía y Geodesia. Facultad de CC. Matemáticas. Universidad Complutense de Madrid. E-28040 Madrid, Spain (aig@eucmos.sim.ucm.es)

[2] Observatorio Astronomico Nacional (IGN), Apartado 1143, E-28800 Madrid, Spain (Burillo@oan.es)

Received 2 May 1996 / Accepted 7 November 1996

Abstract. The edge-on spiral galaxy NGC4013 has been mapped in the J=2–1 and 1–0 lines of ^{12}CO with the IRAM 30m telescope (HPBW 13″and 21″). CO emission is detected within a galactocentric radius, $R \sim 100''$ (5.5 Kpc). The radial molecular gas distribution consists of a ring-like source (of radius $r_{ring} \sim 1.5$ kpc), and a fast rotating nuclear disk (of radius $r_{nucl} \sim 500$ pc).

The CO velocity field, derived from the position-velocity diagram taken along the galaxy major axis, reveals the existence of a compact nuclear disk rotating at high velocities which has no HI counterpart. The derived rotation curve reaches $v_{rot} \sim 130$ kms^{-1} in less than $r \sim 250$ pc. This high velocity regime for molecular gas is satisfactorily explained by an inner bar scenario. The bulge of NGC4013 is box-shaped at optical wavelengths, which suggests the existence of a non-axisymmetric potential in the inner disk. The distribution of CO emissivity itself towards the center suggests that the orbits of some molecular clouds are inclined with respect to the plane of the galaxy.

NGC4013 presents a distorted vertical distribution of matter (stars and gas): it has a box-shaped bulge, a thick optical disk with a warped plane, and a spectacular HI warp in the outer disk. The molecular gas disk vertical structure is not resolved in the 2–1 line. The slight inclination of the galaxy allows us to detect non-axisymmetric structures that are probably spiral arms. If so the estimated inclination angle is i=86.^{o}5, in excellent agreement with the derived by Guthrie (1992) from optical data. We show that the warp of the stellar disk reported from optical measurements might be an artifact due to spiral arms seen in projection. We have not detected a CO counterpart of the HI warp.

Key words: galaxies: individual: NGC 4013 – galaxies: ISM – galaxies: kinematics and dynamics – galaxies: structure – radio lines: galaxies

Send offprint requests to: Ana I. Gómez de Castro

Table 1. Adopted parameters of NGC 4013

Parameter	Value	Source
Center Coor.	α (1950) = 11^h 55^m $57.^s2$	Hummel et al. 1991
	δ (1950) = 44° 13′ 30″	
Pos. Angle	P.A. = 66°	Hummel et al. 1991
Inclination	i = 90°	KS82, Bottema 1995
	i = 85°	Guthrie 1992
	i = 86.°5	This work
Systemic Veloc	V_{Hel} = 835 ± 3 km/s	Bottema 1995;
		This work
Distance	D = 11.6 Mpc	Bottema 1995
Scale	1″ = 55.76 pc	Bottema 1995

1. Introduction

The existence of a hot gaseous halo in many spiral galaxies is now firmly established from observations of radiocontinuum, diffuse H_α, X-rays, absorption by highly ionized gas and other high energy tracers (Hummel et al. 1991; Rand et al. 1992; Pildis et al. 1994; Bregman & Pildis 1994). Recent detections showing the presence of HI chimneys (Heiles 1992), thick molecular disks (NGC891:García-Burillo et al. 1992, hereafter GB; our Galaxy: Dame et al 1987) and dust lanes coming out of the plane (Sofue 1987) support the existence of a strong disk-halo connection also for cold gas.

Different mechanisms have been invoked to explain the existence of gas and dust at large vertical distances from the disks of spiral galaxies. Gas could be driven out of the plane by SN explosions (the so-called chimney models of Norman & Ikeuchi 1989) or radiation pressure (Barsella et al. 1989). Magnetic instabilities could also provide a mean to establish a circulation between the disk and the halo (Foglizzo & Tagger 1995; Matsumoto et al. 1988) and there are indications that they may be acting in the Galaxy at the Gould's Belt scale (Gómez de Castro & Pudritz 1992). Alternatively, this gas might be falling from the intergalactic space in the form of high velocity clouds (Mirabel 1991). Moreover, the excitation of oscillation modes perpendicular to the galactic plane or warps, could push material outside the plane. Near the center of barred galaxies, confirma-

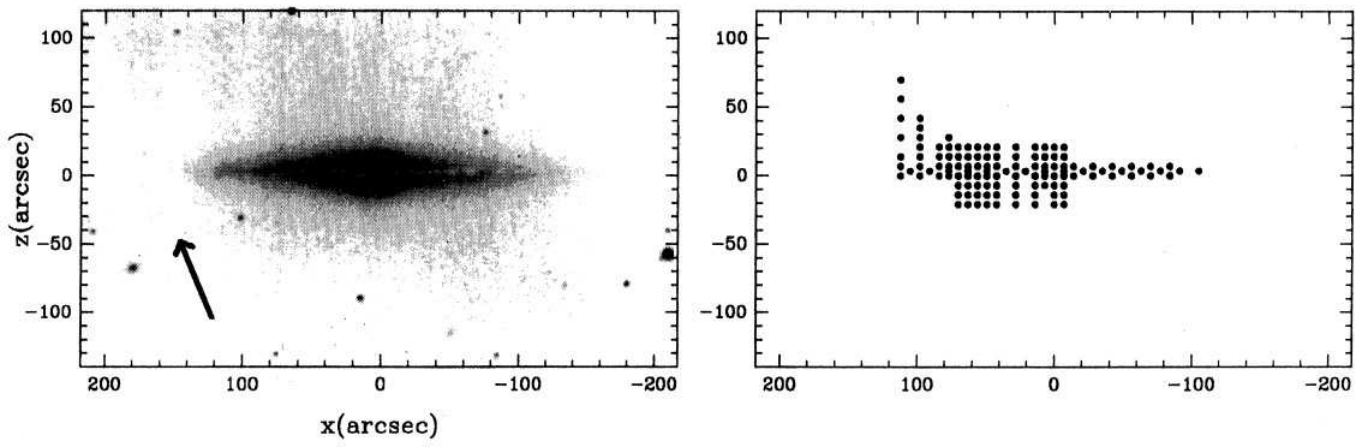

Fig. 1. (**Left**) Optical photograph of NGC 4013 in the Kodal IIIa-F band + Wratten 23A from Bottema (1995); the arrow points to the North. The z and x axes (P.A. -24° and 66°, respectively) are centered in the radiocontinuum source at the galactic center.(**Right**) Grid marking the positions observed with the IRAM 30m telescope (this work).

tion of the existence of orbits coming out of the galaxy plane exists both theoretically and observationally (Heisler et al 1982; Shaw 1993).

In this work we study an edge-on isolated galaxy, the Sbc spiral NGC 4013 (see physical parameters in Table 1). For different reasons this galaxy was thought to be a unique target to study the vertical distribution of molecular gas. First, its aspect ratio, as seen in the optical pictures, indicates that the stellar galactic bulge is box-shaped and unusually thick (van der Kruit & Searle 1982, hereafter called KS and Jarvis 1986). Moreover, NGC 4013 has a 'prodigeous' warp in HI (Bottema 1995; 1996, Bottema et al. 1987), and also a mild warping of the stellar disk has been reported by Florido et al. 1991 from optical observations. A radio continuum halo is detected at 5 Ghz (Hummel et al. 1991, hereafter called HBD). We used the IRAM 30 m telescope to observe the line emission in the 2–1 and 1–0 transitions of ^{12}CO. The high resolution and sensitivity of the 30 m might allow us to resolve the vertical distribution of molecular gas. Moreover, the study of molecular gas is critical in determining both the morphology and evolution of the galactic disk. We present in Sect. 2 the observations, in Sect 3. the results and its preliminar analysis. Sect. 4 summarizes the conclusions of this work.

2. Observations

The ^{12}CO(2-1) and ^{12}CO(1-0) observations were made between September 1993 and January 1994. As an alternative to RA and DEC coordinates we use the x and z axes defined as parallel to the major and minor axes, respectively ($x > 0$ eastwards,and $z > 0$ northwards; a position angle of PA=66° is implicitely assumed in the change of coordinates). The map is centered in the position of the central radio continuum source ((x, z)=(0,0)= (α(1950)=11^h 55^m 57.^{s}2, δ(1950)=44° 13′ 30″) (HBD)).The optical center determined accurately by Palumbo et al. (1988) is at $x = -5''$ and z =3.″5 and it is very close to the dynamical center determined in this work ($x \sim -3''$, z ∼3."5; see Sect. 3.2). The spatial resolving power of the present observations is of 13″ and 21″, for the 2–1 and 1–0 transitions of ^{12}CO, respectively.

The grid of observed positions consists of an ensemble of 3 strips parallel to the x axis and 14 vertical cuts parallel to the z axis. The central x strip samples the galactic plane (with a 14″ x-spacing), goes through the dynamical center (x ∼–3″, z ∼+3.5″) and therefore coincides with the kinematical major axis. The other two strips pass at z=0″ and z =+7″. We made 4 z cuts to partly map the centre of the galaxy. An ensemble of 8 z cuts sampled the possible out of the plane excursions of molecular clouds in a rectangular region Δx x Δz = 55″ x 42″, centered at (x,z) = (56″,0″), in the eastern side of the galaxy. Finally we made 2 strips rising up to high z-distances with z_{max} = 70″ (or 3.9 kpc) at x = 112″ to look for out-of-the-plane CO gas associated with the HI warp (see Fig. 1).

The 30 m telescope was equipped with two SIS receivers (T_R (SSB) = 200–300 K) connected to two 512x1 MHz channel filter banks providing a total velocity coverage of 1332 kms^{-1} in the 1–0 line and of 666 kms^{-1} in the 2–1 line. All the spectra shown in this paper have been smoothed to 13 kms^{-1} and to 10 kms^{-1} for the 2–1 and 1–0 lines, respectively.

All through this work we will express the line temperatures in the T_a^* scale (antenna temperature corrected for atmospheric attenuation and rear sidelobes). For sources of small angular size with respect to the error beam, the main beam-averaged source brightness temperature are derived from T_a^* by T_{MB} = T_a^*/η_{MB}, where η_{MB} is the beam efficiency (η_{MB}= 0.65 at 115 GHz, 0.45 at 230 GHz). The velocity-integrated brightness temperature I(CO) is from $\int T_a^* dv$.

We used as observing procedure a wobbler, with a switch cycle of 4′, avoiding to get CO emission in the reference position. Flat zero to, at most, one order baselines were substracted from the individual spectra.

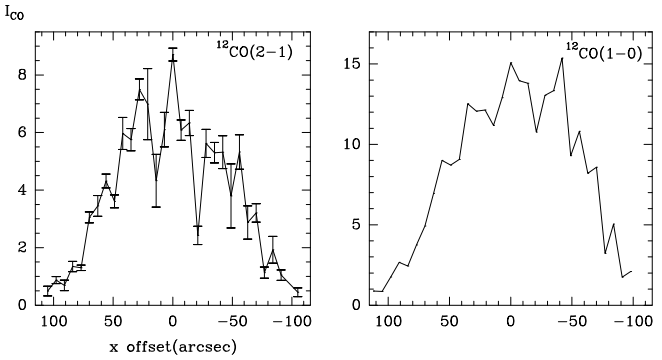

Fig. 2. We represent here the $I_{CO(2-1)}$(**left**) and $I_{CO(1-0)}$(**right**) along the major axis of NGC4013. Units are K Km s^{-1}. Typical error bars are shown in the left panel.

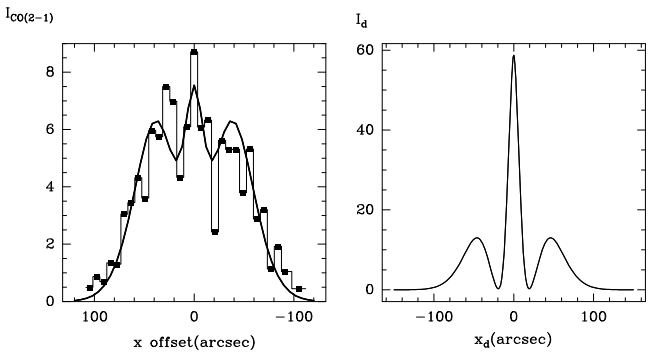

Fig. 3. We overlay on $I_{CO(2-1)}(x)$ (histogram) the fit of an axisymmetrical distribution (thick line) on the left. Units are K Km s^{-1}. The radial distribution deprojected onto the galaxy disk, using an inclination angle of i=$86^o.5$, is shown on the right.

The telescope pointing was monitored by making scans of two bright radiocontinuum sources, 1308+326 and 1156+295, both close to NGC4013, every 1–2 hours during the observations. From the results of the pointing scans we can reasonably estimate a pointing accuracy in our data of $\leq 2''$ rms. Continuum drifts along Jupiter at the beginning of each observing run allowed us to control the telescope focus and beam shape.

3. Results

3.1. The radial distribution of molecular gas

The ^{12}CO(2–1) and ^{12}CO(1–0) velocity integrated intensities observed along the three strips passing at z=0, +3.5$''$ and +7$''$, parallel to the x axis, have been averaged for each x offset to obtain the CO major axis profile ($I_{CO}(x)$) for the galaxy. The results of the averaging are presented in Fig. 2. The CO distribution along the major axis shows an overall symmetry with respect to the center of the galaxy.

At close sight, the in–plane CO emission distribution consists of a 'ring-like' structure (with a radius of $\sim$ 30$''$–40$''$) falling abruptly inwards and more slowly at large radii, and a slightly asymmetrical central nuclear condensation peaking at x=0$''$, that extends from x=+7$''$ up to x=-14$''$ (as it will be shown below the dynamical center is at $x \simeq$ -3$''$). Between the 'nuclear disk' and the 'molecular ring' there is a depression in the I_{CO} radial distribution with minima at x=14$''$ and x=-21$''$. The existence of these three components in the I_{CO} radial profile stands out more clearly in the 2–1 than in the 1–0 line, partly because of the lower angular resolution of the latter.

We have fitted an axisymmetric brightness distribution to the observed $I_{CO}(x)$ radial profile to get the radial distribution deprojected on the galaxy plane, $I_{CO}(R)$. We do not intend to get a detailed fit (the observed distribution is not totally symmetrical), but getting rid of inclination effects allows us to study the average radial distribution in the disk and especially its relation with kinematics and the location of the density wave resonances (discussed in Sect. 3.2). We constrained the fit to simple analytical radial functions: a broad positive gaussian combined with a narrower negative gaussian to account for the 'ring-like' distribution and a very narrow central gaussian for the nuclear disk. In the fitting we have assumed an inclination angle of i=86°.5 (this value is derived in Sect. 3.3). The resulting $I_{CO}(R)$ and the fit to the data, along the major axis, are shown in Fig. 3. The radial distribution of molecular gas in NGC4013 reminds us of that observed in our Galaxy (Dame et al. 1987) and in NGC891 (Sofue et al. 1987; GB; García-Burillo & Guélin 1994, hereafter called GB&G): we distinguish an overall molecular ring distribution with a maximum peak at R$\sim$40-45$''$, a hole between R$\sim$20-40$''$ and a strong maximum at the center. In the general picture of the large-scale distribution of molecular gas in our own Galaxy two main features unveiled by the first CO surveys remain unchanged: the molecular ring and the nuclear disk. The overall distribution shows a large concentration of CO in the galactic center and at radii of 4-8 Kpc; in between there is a relative depression in CO emission.

We have calculated the total molecular gas from the total CO luminosity. For this, we first derived the average velocity-integrated emission along the major axis on a region covering the total x extent of the molecular gas disk ($\sim$ 240$''$) and a z extent of $\sim$ 30$''$, sufficient to get most of the thin disk emission. We have applied a $N(H_2)/I_{CO}$ conversion factor of 2.3x10^{20} H_2 molecules cm^{-2} per K km s^{-1} derived by Strong et al. 1988, to get the total mass. We finally calculated a total molecular gas content of M(H_2)=0.89x10^9 $M_\odot$. According to the determination of Bottema (1995), the total HI mass content is M(HI)=1.3x$10^9 M_\odot$ that leads to M(H_2)/M(HI) $\sim$ 0.69. The total luminous (bulge + disk) mass being $M_{lum} \sim 5.5$x10^{10} $M_\odot$, as reported by the same authors, we get a ratio of the neutral gas content (M(H_2)+M(HI)) to the total mass (M_{lum}) of $\sim$ 0.04.

We have derived an average value of the ^{12}CO(2–1)/(1–0) ratio ($R_{21/10}$) in the disk to test the excitation conditions of the molecular gas. For this, we calculated the average spectrum of the disk in the 2–1 and 1–0 lines, by integrating all spectra (each position being given the same weight) within a range Δx=–110$''$ to 110$''$ and Δz=0$''$ to 7$''$. We obtained an average ratio of 0.65. We have to correct for the different filling factor of the molecular disk within the 2–1 and 1–0 beams

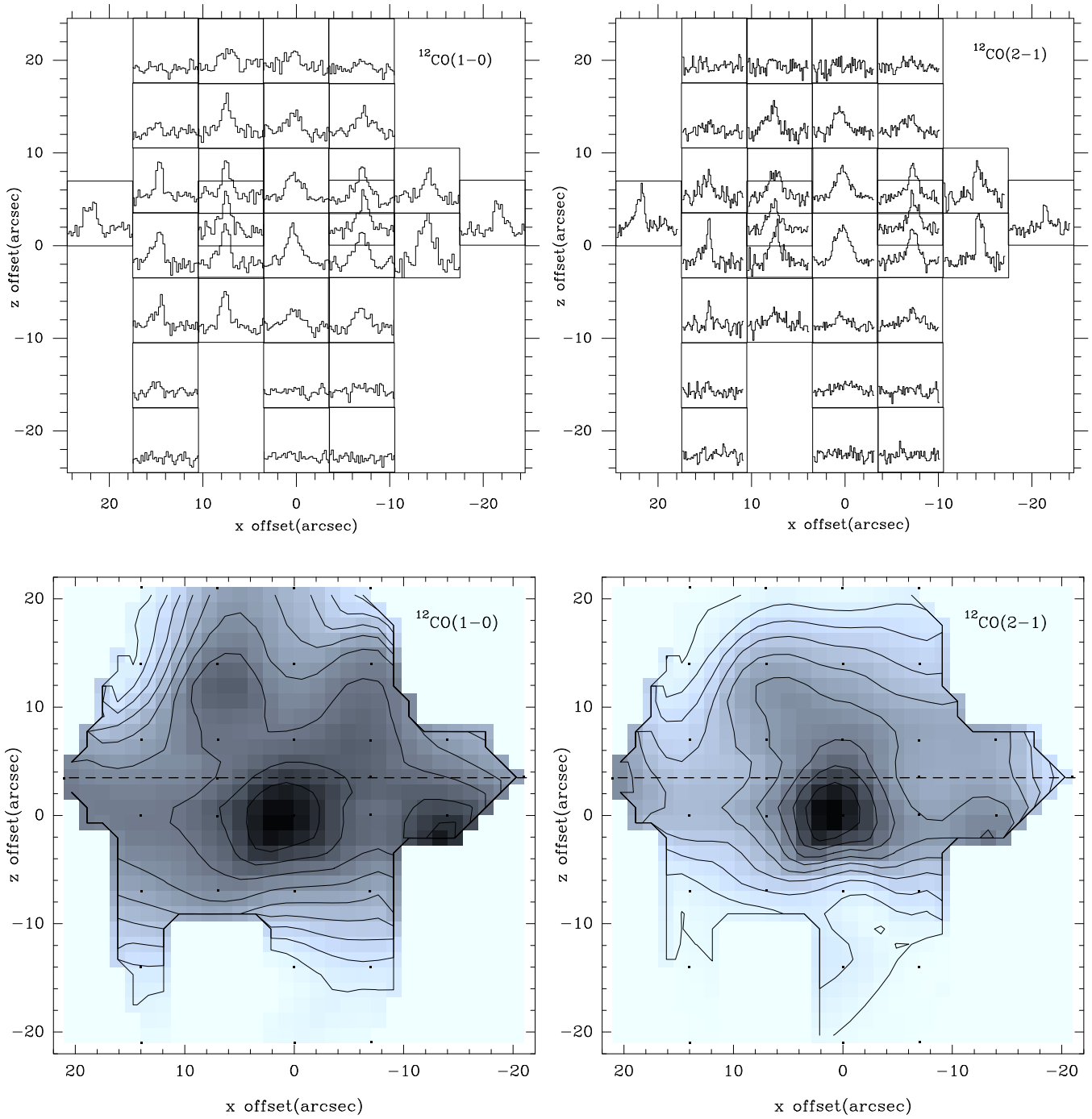

Fig. 4. Top:The ^{12}CO(2–1) (**left**) and ^{12}CO(1–0) (**right**), line profiles in the center of NGC4013. Each profile is represented as a function of the x and z offset in arcseconds. The common velocity scale is 500-1200 Km/s and the temperatures scales (T_a^*) are (-0.025)–(0.075) K for the ^{12}CO(2–1) line and (-0.045) – (0.15) K for the ^{12}CO(1–0) line. **Bottom**: The ^{12}CO(2–1) (**left**) and ^{12}CO(1–0) (**right**) integrated intensity contour maps in the same region shown above. Levels are from 10 to 90% by 10% of the maximum value (9.2 K Km/s for the ^{12}CO(2–1)) line and 16.4 K Km/s for the ^{12}CO(1–0) line. The observed positions are indicated by filled squares.

(f=(FWHM(1-0)+7″)/(FWHM(2-1)+7″) $\sim$ 1.28); where 7″ have been added to the FWHM of the beam to take into account that the values have been obtained by averaging three strips from z= 0″ to z=7″. This rises $R_{21/10}$ to 0.83. In order to study the possible variations of the 2–1/1–0 line ratio in the disk, we have calculated $R_{21/10}$ for each position along the major axis. The differences in resolution along the x axis have been taken into account by smoothing the $I_{CO(2-1)}$ data with a 1-D gaussian of 17″ FWHM. Again, we have multiplied $R_{21/10}$ by f to correct for the different beam filling factors along the z direction. We see no radial trend in $R_{21/10}$. Instead we notice a slight east-west asymmetry: $R_{21/10}$ is on average 0.75 in the western side and it is 0.90 in the eastern side.

3.1.1. The center CO maps

We show in Fig. 4a the 2–1 and 1–0 ^{12}CO line profiles observed towards the center of NGC4013. The corresponding integrated intensity contour maps are shown in Fig. 4b.

In both transitions molecular gas emission seems to come partly from regions out of the galaxy plane. We distinguish four clumps of emission that shape the I_{CO} distribution into a box whose vertexes (**C1**=(7″, 12″), **C2**=(7″, -3.5″), **C3**=(-12″, -3.5″), **C4**=(12″, 12″)) are more or less symmetrically disposed with respect to the dynamical center ((x, z)=(-3″, 3.5″)).

This "molecular gas box" is contained within the "box-shaped bulge" identified in the optical pictures (see Fig. 4b). This nuclear feature extends over Δx=40" and Δ z=22″, according to the photometric studies of KS its existence has been furtherly confirmed in the near infrared picture of Florido et al. 1991 (see also Shaw 1993).

3.1.2. Comparison with other tracers

The relation between the global dynamics of the disk and the radial H_2 distribution as well as the total H_2 mass content starts to be understood. Fig. 5 shows the overlay between the integrated intensity distributions along the major axis seen in HI and in the 2–1 line of CO. We note an anticorrelation between both tracers. The center of NGC4013 is depleted in HI: there is no HI counterpart of the 'nuclear disk' seen in CO. The I_{HI} profile is also 'ring-like' but its maxima lie farther away from the center than in I_{CO} (the HI maxima lie at $x^{HI}_{ring} \sim$ 50″–60″, to be compared with $x^{CO}_{ring} \sim$ 30″–40″). Also, HI is detected along the major axis as far as x$\sim$170″, beyond the optical disk edge (R $\simeq$ 110″ at U=23.58 mag arcsec^{-2}), which coincides in practice with the edge of the molecular gas disk (x$\sim$ 110″).

Molecular and atomic gas apparently avoid each other at large scale, as observed in the radial distributions of many spiral galaxies (NGC891: GB&G; M51: García-Burillo et al. 1993; NGC4565: Neininger et al. 1996). This is probably linked to a change of phase and a radial redistribution of neutral gas, driven by the density wave present in the disk.

Maps of the radio continuum emission have been obtained at 6cm (HBD) and 20cm (Bottema 1995; see also Condon 1987). They show a strong nuclear source and a disk extending up to

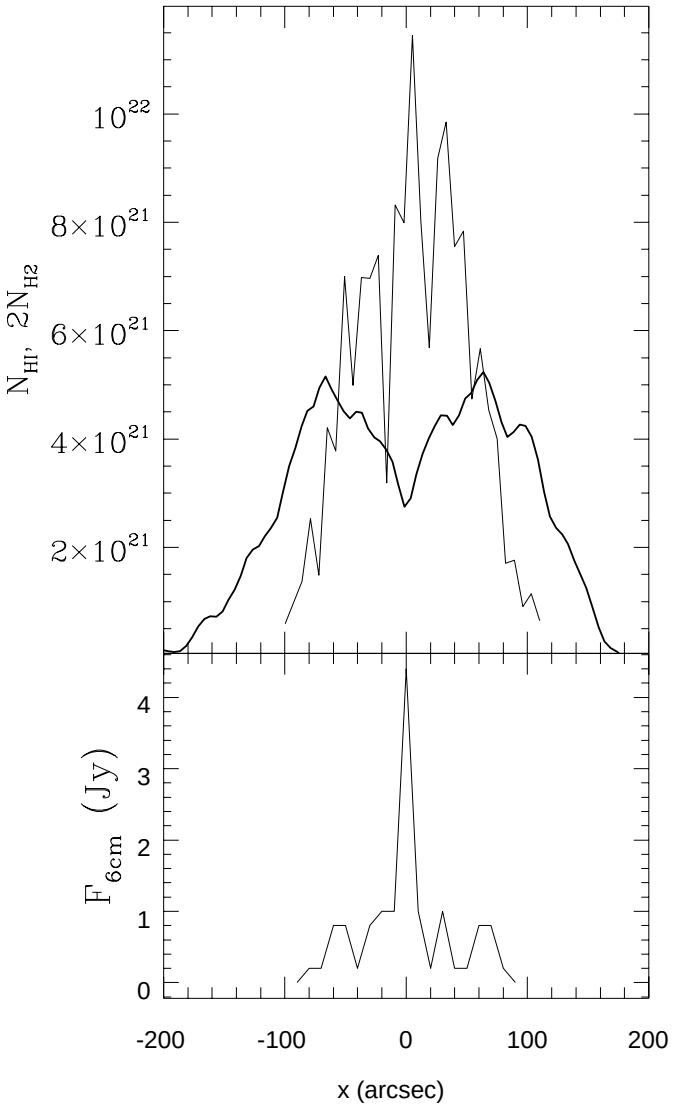

Fig. 5. Top: Column densities of molecular and atomic gas. The column of HI is represented by a thick line and the column of H_2 (multiplied by a factor 2) is represented by a thin line. **Bottom:** 6 cm radiocontinuum intensity from Hummel et al. 1991.

x=$\pm$100″. A close inspection of Fig. 5 reveals also an enhancement of the radiocontinumm emission at R$\sim$20–30″ coinciding with the maxima of the radial distribution of CO. Correlation between nonthermal radiocontinuum and CO emission is observed at large scales in many spirals. This correlation appears in face on spirals, where the spiral arms seen in CO and nonthermal radio continuum overlap nicely, as well as in edge-on galaxies as NGC 4013 where the continuum is integrated along the line of sight. The interpretation of this correlation is still controversial but seems somewhat related to the fact that both are good tracers of massive star formation; CO emision traces the distribution of the large molecular complexes where massive star formation occurs and the supernovae birth rate is larger.

The most outstanding feature in both maps is the unusual large fraction of the nuclear to the disk emission

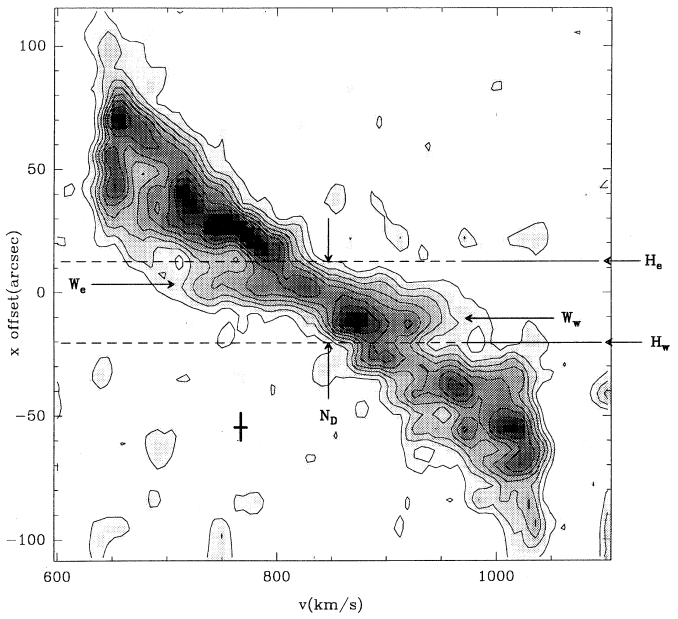

Fig. 6. Position-velocity diagram, observed along the kinematical major axis of NGC4013, in the ^{12}CO(2–1) line (solid contours and grey scale). The location of the nuclear disk (**ND**), the high velocity gas ($\mathbf{W}_e$ and $\mathbf{W}_w$) and the CO depleted regions ($\mathbf{H}_e$ and $\mathbf{H}_w$) are indicated by the arrows. Countour levels and gray scale are equally spaced from 10% to 90% by steps of 10% of the maximum value (0.075 K).

($I_{nuclear}/I_{total} \sim 30\%$) that Bottema (1995) associates with an unusual nuclear activity. The IRAS colours (Rush et al. 1993), the Far InfraRed (FIR) flux (Fullmer & Longsdale 1989) and the mass normalized FIR/1.49 GHz flux ratio (Xu et al. 1994) of NGC 4013 are similar to those of normal galaxies. However the FIR infrared surface brightness is rather large, log(FIR/4R^2_{gal})= -13.8 (see e.g. Pildis et al. 1994), suggesting that there may be an enhancement of the star formation activity in the nucleus of NGC 4013 with respect to other spirals.

3.2. Molecular gas kinematics

3.2.1. The major axis p-v plots

Fig. 6 shows the p–v plot for the 2–1 transition of ^{12}CO (for which the resolution is highest), taken along the kinematical major axis. To synthesize the CO p-v diagram with a high signal to noise ratio, we have averaged the three strips parallel to the major axis (i.e., the strips passing at z=0″,+3.5″,+7″). As NGC4013 is nearly edge-on, Fig. 6 allow us to see the whole expand of velocities and therefore we expect to get a detailed picture of the molecular gas kinematics in the disk. We distinguish two kinematical components:

- In the very inner region (R$\leq$ 10″) there is gas at high projected velocities that shows up by two 'wiggles' on the CO p-v diagram (hereafter we will denote this components as $\mathbf{W}_e$ and $\mathbf{W}_w$, for the eastern and western sides, respectively). The comparison between the nuclear disk seen in $I_{CO}(R)$ and the position of $\mathbf{W}_e$ and $\mathbf{W}_w$ in the p-v plot indicates that they are associated with the same feature.
- An outer region going from R=40″ to R=110″–120″, where the CO gas rotates with the terminal velocity v_{max}=210kms^{-1}.

The dynamical center of the galaxy has been determined by looking at an ensemble of p-v plots parallel to the major and minor axis of the galaxy taken from x=-10″ to 10″ and z=-10″ to 10″. The maximum symmetry in the diagrams is obtained if we assume (x,z) $\sim$ (-5″, 3.5″) to be the dynamical center. A p-v diagram in CO can also be found in Bosma (1994).

The only noticeable difference between the "CO and the HI-based" rotation curves (see Bottema 1995) remains in the inner region: there are no HI counterparts of $\mathbf{W}_e$ and $\mathbf{W}_w$.

The high projected velocity of the gas in the center of NGC4013 may correspond either to gas showing large departures from circular motion or to gas moving at very large circular speed. In case we adopted the HI-based rotation curve (V_{HI}), $\mathbf{W}_e$ and $\mathbf{W}_w$ would be revealing huge non-circular motions. An enhancement of the tangential velocity by a factor larger than 3 (with respect to V_{HI}) is required to account for emission in $\mathbf{W}_e$ and $\mathbf{W}_w$. This is highly unrealistic unless we have an extremely strong gaseous bar. An intermediate solution between pure circular and large non-circular motions, requires that the central mass distribution is non-axisimmetric, i.e. in the shape of a bar or an inner oval (Binney et al. 1991).

The validity of the *bar hypothesis* could be assessed if we detected CO emission from gas circulating at 'forbidden velocities'. We mean by 'forbidden velocities', those that cannot be reproduced by any rotation law but by eccentric elliptical orbits (gas is 'apparently' counter-rotating). No trace of gas emission at 'forbidden velocities' is present in our CO map. We lack of spatial resolution and sensitivity to come to a firmer conclusion. However we do have strong indications suggesting the existence of an inner bar.

Bars are expected to induce large-scale radial flows of gas, creating rings, nuclear condensations and disk regions emptied of gas. The observed radial distribution of molecular gas (I_{CO}(R)) fits within this scenario: it is ring-like and has a strong nuclear disk. Moreover, the outer molecular ring observed in Fig. 3 could be the signature of the 4:1 or -2:1 (i.e., the OLR) resonances of the bar (Combes 1988) Depending on the evolutionary stage of the disk it is expected that that an accumulation of gas occurs in the vicinity of the resonances. Corotation region, however, is progressively emptied of gas (in NGC4013 this region corresponds to $\mathbf{H}_e$ and $\mathbf{H}_w$ in Fig. 6) that feeds the center.

Photometric studies have shown that the bulge of NGC4013 is box-shaped (Jarvis 1986; Shaw 1993). From a theoretical point of view, box- shaped galactic bulges are presently interpreted as a consequence of the resonant action of a central bar potential on the out of the plane excursions of stellar orbits (Heisler et al. 1982; see also Shaw 1993 and references therein). There are certain radii at which the ratio of the frequency of the out of the plane motions of orbits and the frequency of orbital precession is a rational number. Under certain circumstances

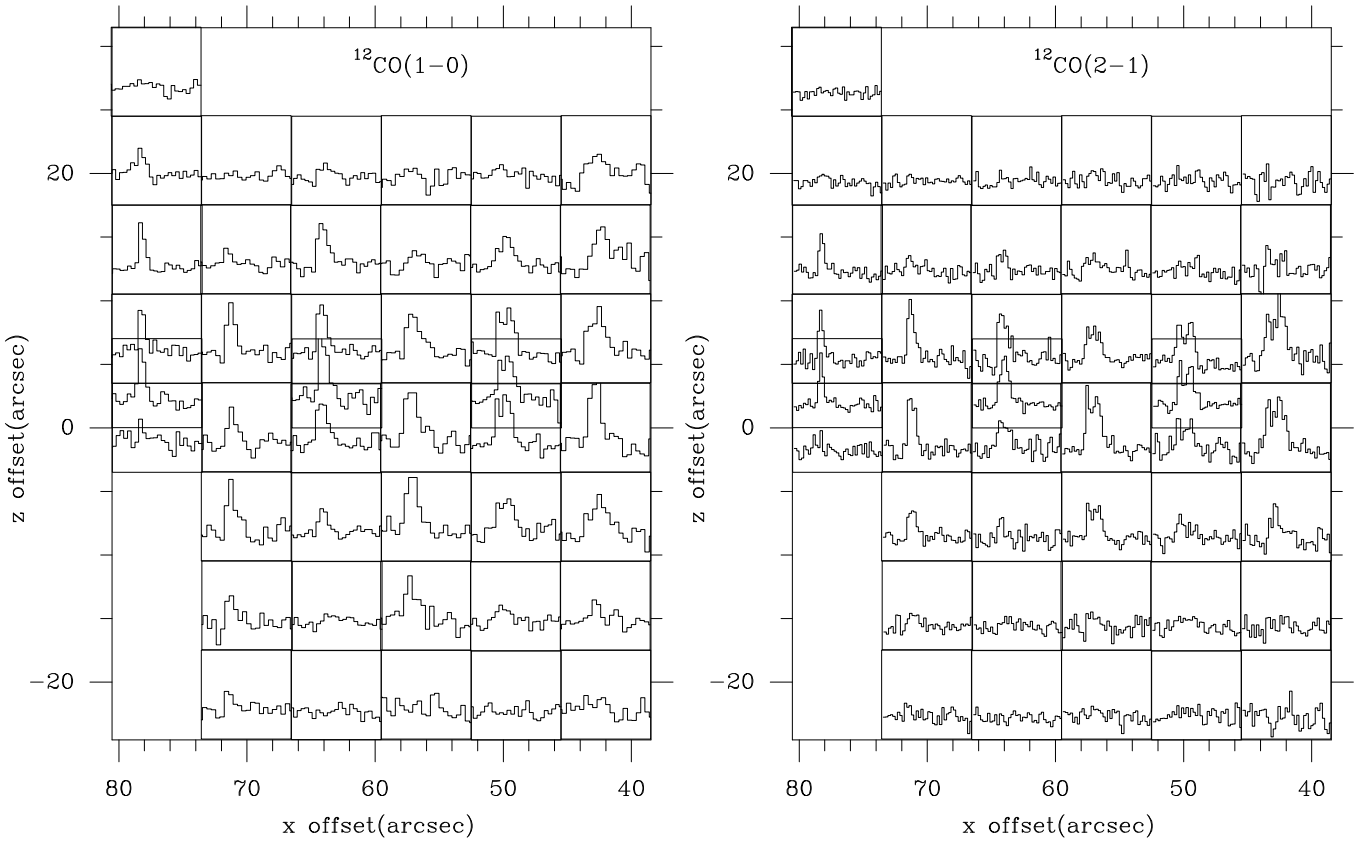

Fig. 7. The ^{12}CO(2–1) (**left**) and ^{12}CO(1–0) (**right**) line profiles observed in the NE side of NGC 4013. The rectangular area mapped is centered at X=59.5″ and Z=0″ and extends over 35″ in X and 40″ in Z. The common velocity scale is 500 – 1000 Km/s and the temperature scales are (-0.025)–(0.075) K for the ^{12}CO(2–1) line and (-0.055)–(0.12) K for the ^{12}CO(1–0) line.

and for a relatively long-lived bar, the bulge tends to thicken at certain radii generating in the long run a box- shaped structure. Therefore there is a link between bars and peanut bulges. The question arises whether there can be a gaseous counterpart for the vertical stellar orbits and especially if these gaseous orbits are either stable or transient.

As it can be seen in Fig. 4a-b., we seem to detect molecular gas out of the galaxy plane in the center of NGC4013. CO emission is distributed in a box-shaped source contained within the limits of its optical counterpart (the so- called 'peanut bulge'). This result suggests that molecular clouds might be describing eccentric orbits inclined with respect to the galaxy plane. According to Fig. 6., these inclined orbits seem to be 'direct' or 'prograde'. Although velocities reached at apocenter might be close to v_{max}, the inclination of the orbits might partly account for a reduction of the "boost" near the center. That would explain why the terminal velocity is not reached in $\mathbf{W}_e$ and $\mathbf{W}_w$.

A detailed high resolution and sensitivity study of gas kinematics in the center of 4013 is clearly needed prior arriving to firmer conclusions. High-resolution (FWHM $\sim 3''$) ^{12}CO(1–0) interferometric observations are in progress and they will be used to ellaborate a complete kinematical model of the center of NGC4013 (García-Burillo et al, in prep.).

3.3. Distribution of CO perpendicular to the disk

As it was stated in the introduction, several tracers of both the stars and the gas seem to indicate that the vertical distribution of matter in NGC4013 is distorted. In particular, a stellar thick disk (KS) and an optical warp (Florido et al. 1991) have been detected. The present analysis has two objectives: (1) to determine the thickness of the molecular gas disk (FWHM$_z$) and (2) to test whether the reported 'optical warp' does represent a real warp of the stellar disk. Note that this distortion could just reflect the presence of a spiral arm seen in projection for a disk that it is not perfectly edge-on. A CO mapping like ours has the advantage of not being affected by overall disk opacity effects because the surface filling factor of molecular clouds along the line of sight, for a given velocity interval, is always very low; the molecular clouds are 'macroscopically' optically thin, although the CO emission lines are optically thick in a standard molecular cloud. Moreover CO provides detailed kinematical information that assess the identification of structures that may not be spatially resolved.

The out of the plane emission of ^{12}CO(2–1) has been mapped in detail in a rectangular area centered at x=59.″5 and z=0″ that extends over 35″ in x and 40″ in z (see spectra in Fig. 7). We first computed the velocity-integrated intensity at each (x,z)

position (I(x,z)=$\int T_a^* dv$). Fig. 8 shows the x-averaged out of the plane distribution of I in this region, I(z)=<I(x,z)>$_x$. The latter can be fitted by a gaussian of FWHM = 18″ plus a long tail to negative z. The deconvolved FWHM$_z$ is 12.″5 (694 pc). We might be tempted to say that we have resolved an abnormally thick molecular gas disk.

We show in Fig. 9 the position-velocity diagram corresponding to the cut perpendicular to the major axis at x = 28″, 42″ and 49″. A close examination of Fig. 9 shows that the thickness measured from I(z) cannot be identified with FWHM$_z$. The CO profiles are clearly double peaked. The peak at the terminal velocity (v$_t$) comes from molecular clouds near the tangential point, therefore it indicates the location of the CO plane. The secondary peak (v$_{sp}$) comes from emission of a non-axisymmetric structure, probably a spiral arm seen in projection. Another possibility is that they do represent large molecular gas complexes really located above/below the plane. The z-shift is particularly dramatic at x =49″ where a CO clump with mass 2.6 $\times 10^7$ M$_\odot$ is located 3.″5 (181 pc) above the midplane position. This mass is 2 orders of magnitude larger than the observed in large molecular cloud complexes outside the plane of our galaxy (Dame et al. 1987). The mass of the clump is of the same order of magnitude than the mass of Dwarf Elliptical galaxies (as Fornax) and an order of magnitude **smaller** than the mass of the large Globular Clusters of our Galaxy (e.g. the mass of M22 is $\sim 6 \times 10^6$ M$_\odot$). The energy required to keep this mass lifted above the plane is enormous. An intriguing possibility is that this energy is provided by the impact of High Velocity Clouds; this possibility has been suggested for the Big Dent, a galactic nearby star formation supercomplex with a total mass of $\sim 10^7$ M$_\odot$ (see Alfaro et al. 1991). However the total mass of molecular gas associated with the Big Dent is of only $\sim 3 \times 10^6$ M$_\odot$, still ten times smaller than the mass of the CO clump. Therefore we think that the clumps are most likely associated with spiral arms. Using the rotation curve derived in Sect. 3.2 and the observed radial velocity (v$_{sp}$) of the the spiral arm, we derive an inclination angle of the plane of i=86.^{o}5. Our value agrees satisfactorily with the inclination inferred by Guthrie (1992) who determined the axial ratio of NGC4013 from the analysis of a blue P.O.S.S. plate.

To get rid of the bias due to inclination effects on the derived value of FWHM$_z$, we must evaluate the latter for each velocity component separately. The z profiles corresponding to the arms pasing by x = 42″ and x = 56″ can be well fitted by gaussians with FHWM $\sim$ 15″ and henceforth the thickness of the CO gas layer in the spiral arms is only marginally resolved. This is not surprising, since the scale height of the molecular gas in the thin disk component of the Galaxy is typically 60-100 pc (see e.g. Sanders et al. 1984, Clemens et al. 1988; Bronfman et al. 1988).

The detection of spiral arms in this region also suggests that the reported mild warping of the stellar disk may just be a misidentified spiral arm seen in projection. The optical warp is best observed in the U Johnson band that traces the distribution of the young stellar population in the disk. It runs towards positive z from x =60″ to x =100″ and then bends back to the plane reaching negative z at the edge of the optical disk. We have found kinematical signatures of spiral arms in the inner part of this area: $x \leq 70''$ (see Fig. 7) (further out I$_{CO}(x)$ declines rapidly). This interpretation of the optical data has the additional advantage of providing a natural explanation for an otherwise rather puzzling characteristic of the optical warp. The optical warp is best traced by the young stellar population (U-band) and runs in the opposite direction than the HI gas warp.

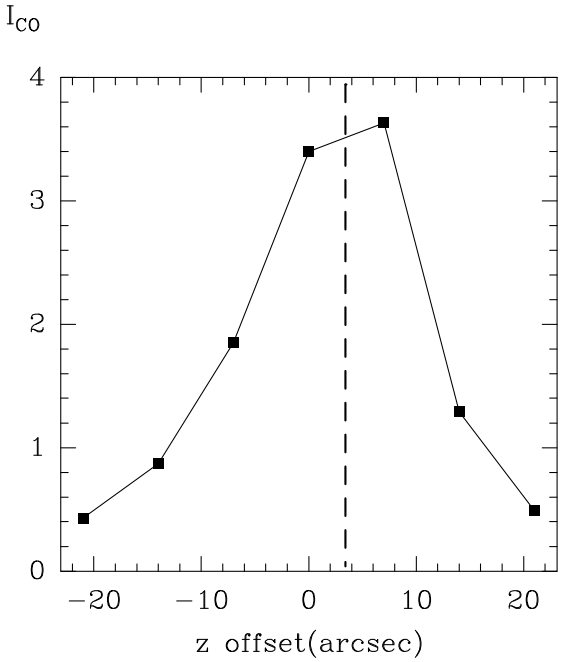

Fig. 8. The ^{12}CO(2–1) mean z distribution in the region between x =42″ and x=70″. Units are K Km s^{-1}. The dashed corresponds to the major axis locus.

Finally, we have made several scans towards high Zs at x=77″,84″,98″ and 112″ without detecting out of the plane emission that could be associated with the HI warp. Neininger et al. 1996 have shown that also for the edge-on spiral NGC4565 the CO emission is constrained to the optical disk and that henceforth does not show up in the HI warp. Continuum dust emission, however, is observed to follow the warp NW edge of NGC4565. Neininger (private communication) also reports the detection of the NGC4013 warp in the 1.2 mm continuum dust emission.

4. Summary and conclusions

In this work we analyze the molecular gas emission of NGC 4013 with a spatial resolution of 13″ and 21″ in the ^{12}CO(2–1)and ^{12}CO(1–0)lines respectively. The main result of this work is the discovery of a molecular gas nuclear disk showing high rotation velocities. The CO-based rotation curve reaches 130 kms^{-1} in less than $r \sim$ 250pc. This gaseous compact source is to be linked with the box-shaped bulge apparent in optical wavelengths and it is the signature of a molecular gas bar. It is also suggested that a fraction of molecular clouds in the inner disk start to leave the plane describing slightly inclined

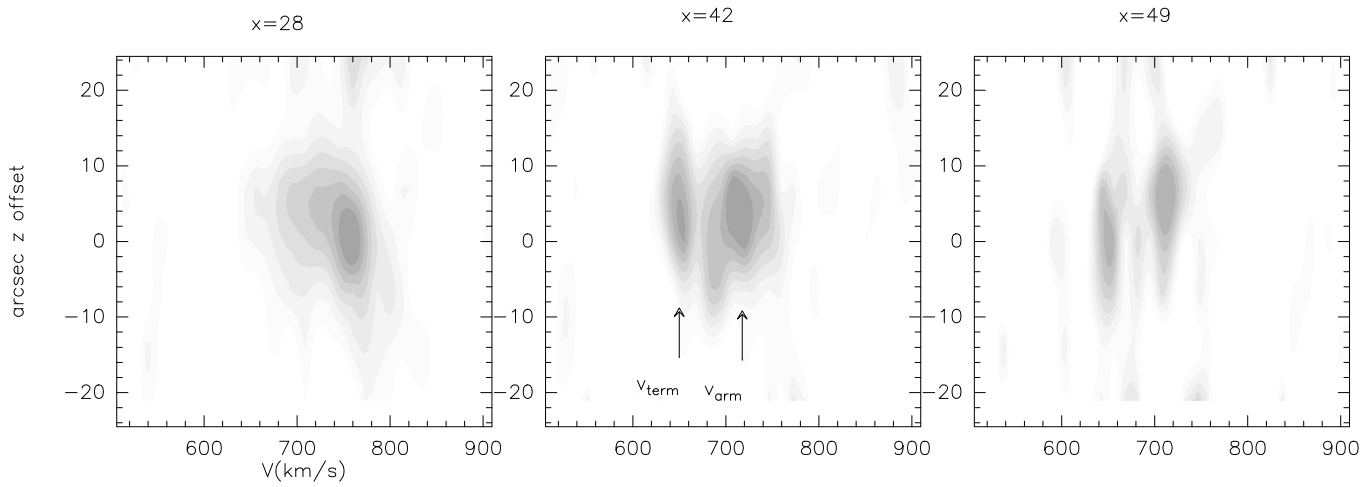

Fig. 9. The ^{12}CO(2–1) p-v plot corresponding to the cut perpendicular to the major axis at $x = 49''$. v_t and v_{sp} denote the position of the gas at the terminal velocity and the spiral arm, respectively. Gray scale levels are equally spaced from 10% to 90% by steps of 10% of the maximum value (0.06 K).

eccentric orbits. The orbits seem to be prograde (or direct) and are likely induced by the vertical resonance close to the inner Lindblad resonance of a barred potential. Moreover, we have found that,

- The in-plane distribution consist of a ring-like structure with a maximum peak at R $\sim 40''$-$45''$, a hole between R$\sim 20''$-$40''$ and a strong central peak. The CO emission decreases gently in the outer borders of the disk up to R $\sim 112''$ where it fades away. The total molecular gas content of NGC 4013 is M(H_2) = 0.89 $\times 10^9$ $M_\odot$ that leads to a M(H_2)/M(HI) $\sim$ 0.69.
- There is a slight east-west asymmetry in the radial distribution of CO and other tracers (HI and 5GHz radiocontinuum) that is also observed in the excitation of the molecular gas: the $R_{21/10}$ is smaller in the western side.
- NGC 4013 is not perfectly edge-on. Its slight inclination produces an artifictial widening of the projected disk thickness. This shows up clearly when the spatial and the kinematical CO data are analyzed altogether. As a consequence, it is shown that the vertical structure of the CO disk is unresolved. Several clumps likely associated with spiral arms are observed at different z because of the slight disk inclination that is determined to be 86.°5. This inclination affects previous estimates of the scale height of the stellar disk (KS).
- The optical warp found by Florido et al. 1991 is more likely a misidentified spiral arm seen because the slight inclination of NGC 4013. We confirm that CO is the best tracer to study the spatial distribution of the young population.
- We have not found molecular gas associated with the HI warp.

Finally, we must stress that high-resolution (FWHM $\sim 3''$) ^{12}CO(1–0) interferometric observations are instrumental to ellaborate a complete kinematical model of the center of NGC4013. The observations are in progress and they will be presented in a forthcoming paper together with a detailed dynamical study (García-Burillo et al, in prep.).

Acknowledgements. We thank the Pico de Veleta staff for their valuable help during the observations. This work has been partially supported by the Spanish CICYT under grant number PB93-0408 and PB93-0491. We thank Roelof Bottema who very kindly provided us the HI data of NGC 4013. We wish to thank Eduardo Battaner, Francoise Combes, Estrella Florido, Michel Tagger and Lourdes Sanz for stimulating conversations.

References

Alfaro, E.J., Cabrera-Caño, J., Delgado, A.J., 1991, ApJ, **378**, 106
Barsella, B., Ferrini, F., Greenberg, J.M., Aiello, S., 1989, ApJ., **209**, 349
Binney, J., Gerhard, O.E., Stark, A.A., Bally, J., Uchida, K.I., 1991 M.N.R.A.S., **252**, 210
Bosma, 1994, NATO ASI on the "Opacity of spiral discs", preprint of the Observatoire de Marseille.
Bottema, R., Shostak, G.S., van der Kruit, P.C., 1987, Nature, **328**, 401
Bottema, R., 1995, A&A, **295**, 605
Bottema, R., 1996, A&A, **306**, 345
Bregman, J.N., Pildis, R.A., 1994, ApJ, **420**,570
Bronfman, L., Cohen, R.S., Alvarez, H., May, J., Thaddeus, P., 1988, ApJ, **324**, 248
Clemens, D.P., Sanders, D.B., Scoville, N.Z., 1988, Ap J, **327**, 139
Combes, F., 1988 NATO ASI Series C, 232, 475
Condon, J.J., 1987, ApJS, **65**, 485
Dame et al. 1987, ApJ, **322**, 706
Florido, E., Prieto, M., Battaner, E., Mediavilla, E., Sánchez-Saavedra, M.L., 1991, A&A , **242**, 301
Foglizzo, T., Tagger, M., 1995, A&A, **301**,293
Fulmer, L., Lonsdale, C., 1989, Cataloged Galaxies and Quasars Observed in the IRAS Survey, Version 2, Pasadena, JPL **242**, 301
García-Burillo, S., Guélin, M., Cernicharo, J., Dahlem, M., 1992, A&A, **266**, 21
García-Burillo, S., Guélin, M., 1995, A&A, **299**, 657
Gómez de Castro, A.I., Pudritz, R.E., 1992, ApJ, **395**,501

Guthrie, B.N.G., 1992, AAS, **93**, 255
Heiles, C., 1992, Evolution of Interstellar Matter and Dynamics of Galaxies, p. 12, Eds. J. Palous, W.B. Burton and P.O. Lindblad, Cambridge University Press.
Heisler, J., Merritt, D., Schwarzschild, M., 1982, ApJ, **258**, 490
Hummel, E., Beck, R., Dettmar, R.-J., 1991, AAS, **87**, 309
Jacobi, S., Kegel, W.H., 1994, AA, **282**, 401
Jarvis, B.J., 1986, AJ, **91**, 65
van der Kruit, P.C., Searle, L., 1982, Astron. Astrophys., **110**, 61
Matsumoto, R., Horiuchi, T., Hanawa, T., Shibata, K., 1988, PASJ, **40**,171
Mirabel, I.F., 1991, Proceedings IAU 144, p.89
Neininger, N., Guélin, M., García-Burillo, S., Zylka, R., Wielibinski, R., 1996, A&A, in press
Norman, C.A., Ikeuchi, S., 1989, Astrophys.J., **345**, 372
Palumbo et al. 1988, Accurate positions of Zwicky galaxies, October 1988 Special version. Includes 1987 AAS, **70**, 189 and additional measurements.
Pildis, R.A., Bregman, J.N., Schombert, J.M., 1994, ApJ, **427**,160
Rand, R.J., Kulkarni, S.R., Hester, J.J., 1992, ApJ, **396**,93
Rush, B., Malkan, M.A., Spinoglio, L., 1994, ApJS, **89**, 1
Sancisi, R., Allen, R.J., 1979, A&A, **74**, 73
Sanders, D.B., Solomon, P.M., Scoville, N.Z., 1984, ApJ, **276**, 182
Shaw, M., 1993, MNRAS, **261**, 718
Sofue, Y., 1987, PASJ, **39**, 547
Sofue, Y., Nakai, N., Handa, T., 1987, PASJ, **39**, 47
Strong, A.W., Bloemen, J.B.G.M., Dame, T., Grenier, I.A., Hermsen, W., Lebrun, F., Nyman, L.A., Pollock, A.M.T., Thaddeus, P., 1988, Astron. Astrophys., **207**, 1
Xu, C., Lisenfeld, U., Volk, H.J., Wunderlich, E., 1994, AA, **282**, 19

This article was processed by the author using Springer-Verlag LaTeX A&A style file *L-AA* version 3.